

# High Resolution Thermal Imaging on a Small Satellite

Mike Goddard, Steven Knox, Harbinder Rana, James Bell, John Gilby, Diego Angarita-Jaimes, Trevor Wood, Calem Whiting, Nigel Philips, Matthew Price, Alan Matthews, Grant Childs, Tony Pattison, Mark Cantrill, Rupert Taylor, Jonathan Karimian, Andrew Haslehurst, Alex da Silva Curiel, Sir Martin Sweeting.

Surrey Satellite Technology Ltd (SSTL), Tycho House, 20 Stephenson Road, Surrey Research Park, Guildford GU2 7YE, United Kingdom. [acuriel@sstl.co.uk](mailto:acuriel@sstl.co.uk)

## ABSTRACT

Technology has advanced rapidly in recent years making high resolution thermal imaging viable for emerging commercial applications. The “DarkCarb” instrument has been specifically designed to provide high-resolution thermal video imagery from a small satellite in support of a range of emerging commercial, government and scientific applications. So far, such capability has only been available on large expensive satellites in a very limited fashion. Sensor and cooling technologies have evolved in recent years so that such an instrument can now be designed and operated to provide useful performance over a typical satellite design-lifetime, and at a cost making new applications financially viable. The instrument provides 3.5 m Ground Sampling Distance (GSD) over a 4.5 x 3.6 km scene with an average Noise Equivalent Temperature Delta (NETD) of between 60 mK and 70 mK depending on viewing conditions and provides the capability to differentiate between objects and surfaces of different temperature and emissivity. Machine learning and automation have made the use of Earth Observation (EO) data increasingly valuable across a range of emerging applications. Thermal imaging can complement daytime visible imagery with additional detail that can be observed in thermal bands, and at night can be more cost effective than Synthetic Aperture Radar (SAR) imaging. Thermal imaging can help in identifying hotspots, industrial activity, support climate change applications, and monitor patterns-of-life. Thermal imaging has additional application in Space Situational Awareness. This paper provides an overview of the DarkCarb spacecraft and instrument, documents its ground qualification and in-orbit validation and results following its launch in June 2023.

## Introduction

Surrey Satellite Technology Ltd. (SSTL) is one of the pioneers in small satellites and started developing innovative Earth Observation missions 40 years ago

been at the forefront of small satellite design and innovation. With over 70 small satellites launched, ranging in applications from Earth Observation, Communication, Navigation, Science and Technology Demonstrations, SSTL has gained invaluable experience using a flexible design approach and rapid development thereby delivering reliable satellite missions at low-cost and within short timescales.

## The Market

The 2010-2020 period saw demand for EO data increasing significantly, building on opportunities in agriculture, surveillance, and big data analytics. Numerous NewSpace companies were established to leverage small satellite technology to address this market, and temporal resolution would give small satellite an edge over the more established institutional and commercial EO systems. As the EO market for imagery and value-added products grew, Planet, BlackSky, Satellogic, Axelspace, Head Aerospace and a few others have since largely addressed the optical imaging market, and IceEye, Capella, Synspective, and Umbra have started addressing the SAR market in a similar way.

There are still a range of applications where there is market demand and/or market potential, for instance in environment monitoring, crop health, greenhouse gas monitoring, but where performance of existing technology would not permit a viable small satellite system to be implemented.

MWIR and TIR sensors in particular have been part of many institutional missions including Landsat and Sentinel and provide relatively poor resolution in support of long-term mapping applications. With advances in MWIR and

TIR sensors, partially driven through demand during the Covid-19 pandemic, several NewSpace service providers have been investigating potential markets based on what these COTS devices can offer. A few companies, including OraraTech, HydroSat, Constellr have started to leverage these capabilities to provide modest spatial resolution thermal imaging. More recently also Supersharpe and Albedo are considering higher resolution thermal imaging capabilities.

Within SSTL, its engineers realised that with these recent advances in sensor technology, long-life coolers, and coupling these with the target tracking video imaging Carbonite series of small satellites, it would become possible to develop a high-resolution thermal imaging satellite with video capability. This “SSTL-DarkCarb” spacecraft would be able to address a range of interesting and emerging applications, including night-time surveillance and climate change applications. Satellite Vu (now SatVu) then teamed with SSTL as the sponsor, with the aim to develop “the world’s thermometer in space”

## The Carbonite Series

As the market moved towards small satellite constellations and the desire for multi-spectral data grows, demand for low-cost and reliable spacecraft offering a range of sensors, has been increasing. SSTL, building on experience gained in the small satellite and constellation business, as well as innovative ‘miniaturisation’, has developed a series of spacecraft to meet the needs of this expanding market. Based on the low-cost Carbonite series of platforms, SSTL has designed three highly innovative, and in some cases ground-breaking, satellites (C. Weiss et al.)

- Carbonite – 1 m resolution optical imager in the visible range
- DarkCarb – 3.5 m mid-wave infrared (MWIR) imager
- CarbSAR – 0.5 m X-band synthetic aperture radar (SAR) imager

More recently SSTL has also been looking at a SWIR and TIR bands, based variant in this series of spacecraft, with the aim to support applications in hyperspectral imaging, including monitoring greenhouse gas emissions, vegetation health and land surface temperature.

## The Carbonite Platform

The DarkCarb satellite is based on SSTL’s Carbonite series of platforms – small, ultra low-cost, capable, platforms designed and built for rapid-delivery (N. Navaranthinam et al.) with Carbonite-1 first launched in July 2015. Carbonite-1 was the first-generation satellite on a roadmap to develop a new product at a low price point and deliver high resolution imagery and video within a shortened delivery schedule. Built in just 6 months, it applied SSTL’s experience and design approach to exploit new, commercially developed technologies, protocols and processes, extensive use of commercial off-the-shelf (COTS) components, and SSTL’s automated production capabilities to deliver a high utility satellite providing high resolution imagery. It also demonstrated the use of video imagery acquired from space, opening up a whole new range of applications to the commercial sector. Carbonite-2, the second technology demonstrator in the Carbonite series, was launched in January 2018 and introduced several design improvements and additional experiments.



*Fig. 1. Carbonite-2*

Carbonite-1 and Carbonite-2 established a standard for high utility satellites at low cost and short schedule but were designed as technology demonstrators.

## The DarkCarb Platform

The current iteration of the Carbonite platform being used on DarkCarb is the next step in the programme – a commercial offering building on the experience and technological advancements of the first two platforms. It features a number of enhancements compared to its predecessors to provide superior performance and functionality and reduces costs and schedule through manufacturing improvements. Some of the new platform features include:

- SSTL's latest suite of core avionics which combines previously separate OBC, AOCS, GPS, and TT&C receiver and transmitter functionality into a single module. This has the advantage of significantly reducing mass and volume, as well as improving power consumption, allowing more power to be allocated to payload operations.
- Next generation data recorder, the HSDR-X, which combines a high-speed data recorder and mass memory unit with embedded X-band exciter functionality, based on previous SSTL technology (D.Cooke et al.). The HSDR-X offers a reduction in mass, volume, power, and cost, and an increase in capacity and bandwidth, with 500 GB of storage. The integrated RF architecture introduces flexibility in the RF solution, allowing variable modulation schemes and data rates with no hardware changes. The baseline data rate is 500 Mbits/s with potential for up to 1 Gbit/s or more, depending on the modulation scheme used.
- Water propulsion system capable of providing more than 130 m/s delta-V, allowing the selection of lower orbits to improve GSD, and other orbital manoeuvres such as altitude maintenance or phasing. The water-based system reduces launch site handling costs and schedule, and the module nature of the propulsion system means the number of tanks can be altered depending on customer requirements.
- Increased redundancy. The avionics and payload chain (excluding the imager and detector electronics) are fully redundant, with an electrically redundant propulsion system.
- Automated LEOP following separation from the launcher. Minimal operator intervention will be required to get the satellite to a de-tumbled, power and thermally safe attitude, reducing cost and commissioning time.

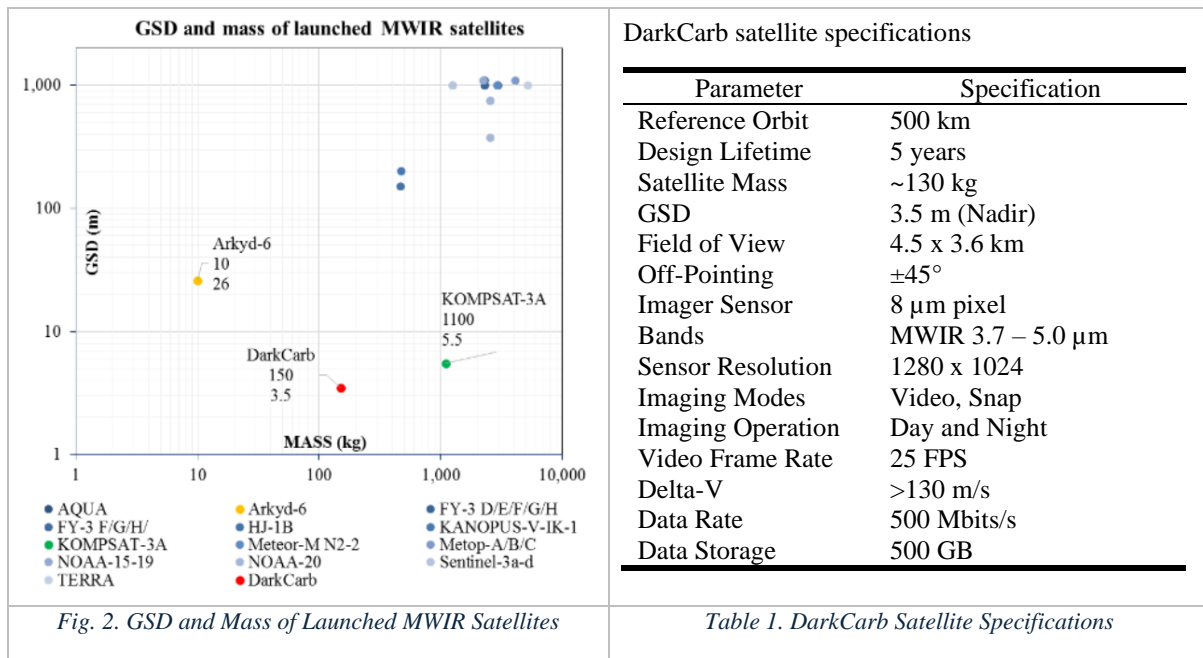
The platform uses a forward-motion compensation (FMC) mode which allows the satellite to point and stare at a particular location over a prolonged period of time; this mode is used to capture still images or video up to 25 frames per second (FPS), providing up to 60 s of video for a particular target at extreme roll angles. The platform is also agile, capable of moving from one target to another over roll angles of up to  $\pm 45^\circ$ .

## DarkCarb Satellite

### Overview

DarkCarb is a highly innovative satellite designed to fill a gap in the EO market by providing MWIR imagery at low cost and high resolution. MWIR imagery provides several advantages over visible imagery, including the ability to image both night and day under any lighting condition, providing additional temporal information by comparing temperature changes on a still target, and using temperature information to monitor items otherwise invisible to visible sensors.

The current commercial market for MWIR imagers is a trade-off between mass and resolution – the higher resolution platforms typically have masses greater than 1,000 kg, as seen in Fig. 2. SSTL decided to approach this market with the same 'smallsat mentality' and flexibility design approach which has been so successfully applied to its current range of EO satellites.



The payload is based on a Mercury Cadmium Telluride (MCT) cooled, 8 μm pixel detector and provides a 3.5 m GSD (at 500 km) and FOV 4.5 x 3.6 km. The detector produces imagery in the 3.7 – 5.0 μm MWIR waveband and has an average NETD of 30 mK. The top-level specifications for the DarkCarb satellite are shown in Table 1 below.

## HotSat-1 and DarkCarb Applications

MWIR imagery provides some key differentiators from visible imagery and combined with the capabilities of the DarkCarb platform the applications are wide-ranging. MWIR imagery will provide the capability to differentiate between objects and surfaces of different temperature and emissivity, providing complementary information to traditional visible imagery and the ability to extend imaging opportunities into nighttime, as well as different lighting conditions in daytime imaging.

DarkCarb can provide utility in the mapping of heat islands in urban areas, including the detection of buildings or installations emitting a significant level of heat, to support environmental activities or detecting waste and pollution spills or discharge from sewage plants and power plants, assuming the pollutants are warmer than the surrounding water bodies.

Satellite-Vu commissioned SSTL for the manufacture and launch of HotSat-1, with Kick-Off at the end of 2021. Development and build continued through 2022, with final Spacecraft testing taking place in early 2023 before launch in June 2023.

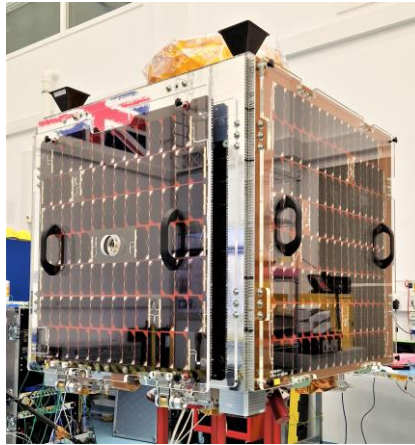


*Fig. 3. HotSat-1 Prior to Leaving SSTL*

DarkCarb also has the potential to assist with disaster support activities for wildfires, volcanic eruptions, and flooding, for example, and may also provide utility in urban areas to support environmental activities that are threatening our world today through the detection of buildings or installations emitting a significant level of heat.

The video generation capability adds unique advantages over traditional MWIR imagery, allowing the detection of highly dynamic features in scenes to be provided and extracted, such as 3D profiles, movement tracking, and speed measurement. Frames can also be stacked to provide improved image quality.

## DarkCarb Constellation Possibilities

The current trend in the EO market is to deploy large constellations of satellites in order to achieve high temporal resolution and global coverage. The low-cost nature of the design makes the DarkCarb satellite ideal for a multi-satellite constellation, allowing users to build up a large constellation for rapid-revisit. The platform's low mass and volume means multiple satellites can potentially be launched at the same time, allowing a full constellation of different platforms to be operational within months.

As the market moves towards small satellite constellations and the desire for multi-spectral data grows, demand for low-cost and reliable spacecraft offering a range of sensors, by themselves or in groups, has also been increasing. Multi-sensor constellations provide the capability to maximise the advantages of each sensor type by combining the different data sets to increase the content and improve the accuracy of available information from a particular target or location of interest. DarkCarb would add considerable value to a mixed sensor constellation – allowing data collection to be extended into nighttime providing interesting possibilities for data fusion for a wide range of applications, potentially not accessible before due to the large and costly nature of previous MWIR imaging satellites.

## DarkCarb Payload

### Optical System

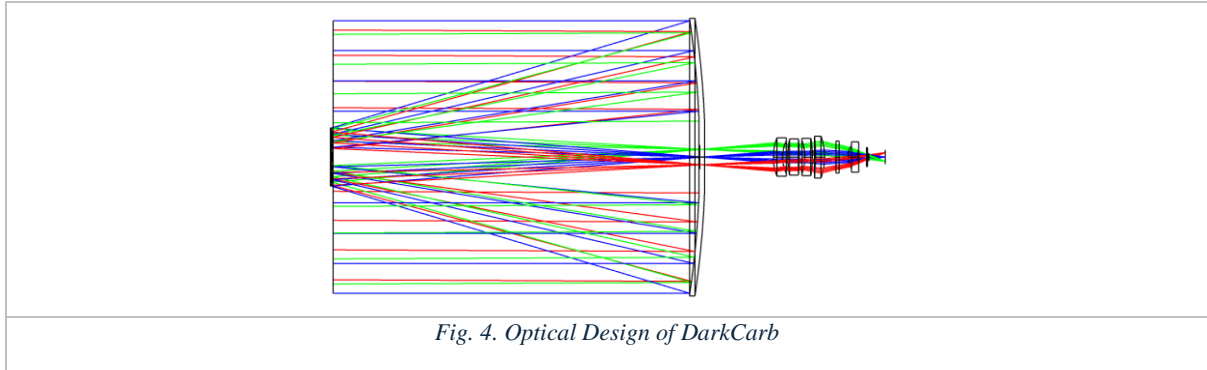
The DarkCarb imager has been optimised to produce high resolution imagery in the MWIR waveband from 3.7 to 5.0  $\mu\text{m}$  with a GSD of 3.5 m from an orbit of 500 km. The detector is an MCT-based 8  $\mu\text{m}$  pitch device with a format of 1280 x 1024 placed in an f/2.8 dewar connected to an active linear cryogenic cooler operating at 110 K.

The imager optical design is based on a Ritchey-Chretien telescope that is coupled to a relay lens assembly. The relay lens assembly re-images the optical system stop at the Secondary Mirror onto the detector dewar cold shield.

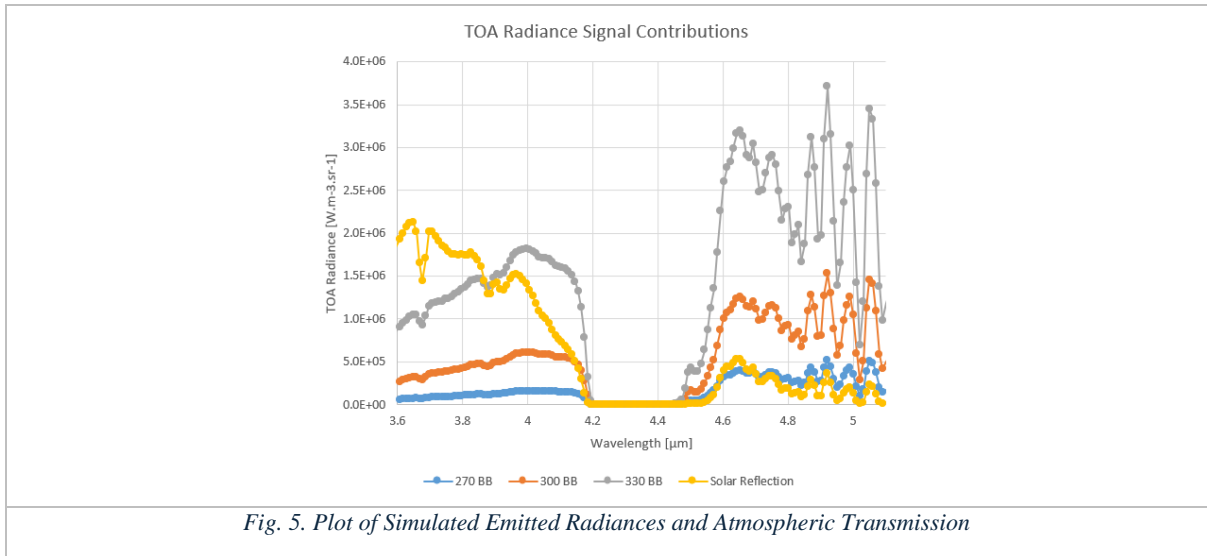
The dewar cold shield has an optical speed of f/2.8m however in order to reduce the telescope aperture and thus mass and volume of the imager while meeting the focal length requirements, an f-number mismatch has been

applied (Gat et al.). In this case, the optical system optical speed has been reduced to f/3.6 (clear aperture of 316 mm) and the dewar cold shield is re-imaged onto the Secondary Mirror, which has been reduced in size to match the f/3.6 in speed. The f/2.8 optical speed (an over-aperture at the Secondary mirror) of the dewar is catered for by using a low-reflectivity annulus mounted around the Secondary Mirror, also known as the Secondary Cold Shield. This Cold Shield minimises any reflections that may lead to stray light, and as the name suggests the shield is cooled in order to reduce any Thermal Self Emission.

Thermal modelling suggests that the Secondary Cold Shield only needs to be cooled down to -20°C rather than matching the dewar cryogenic temperature of 110 K. The optimised relay lens assembly ensured the only non-optical surface producing thermal emission in view of the detector is the Secondary Cold Shield. While being passively cooled with the use of a radiator viewing cold-space, it ensures the contributions to stray light caused by the f-number mismatch have a near-negligible impact on the NETD of the system.



The imager has been designed for nominal operation on the eclipse side, i.e. nighttime operation, and in this case detect the full MWIR waveband of the detector. Fig. 5 shows the Top-of-Atmosphere (TOA) radiances for the reflected solar signal, and for Blackbodies at 270 K, 300 K and 330 K. These assume a US Standard 1976 Urban atmospheric transmission model, which shows the CO<sub>2</sub> band block between 4.2 and 4.5  $\mu\text{m}$ . The Solar Reflection contributions assume an Albedo of 0.3, and a Solar-Zenith-Angle of 45°.



This demonstrates the impact the reflected solar energy has on the overall signal level at the aperture of the telescope, and when compared to the contributions from the ground targets of various temperatures (assuming 100% emissivity), an appropriate compromise during daytime imaging would be to utilise the CO<sub>2</sub> band block of the atmosphere and place a filter in the optical system to block the contributions below 4.2  $\mu\text{m}$ . Note the atmospheric radiance contribution to the signal has not been included in the figure but is of a much lower intensity.



With the filter required for daytime imaging, during nighttime imaging an equal-length window is required for the performance of the optical system to be maintained – the accommodation of this filter and window is discussed in Section 0

## Mechanical System

The requirements that the optical system demands from the imager structure are largely typical for an imager, with some specific and unusual features, to be achieved in the context of being able to support flexible design and rapid manufacture at a commercial cost point.

For any imager, the regulation of the primary to secondary (M1-M2) separation is crucial to maintaining the focused image coincident with the detector, and the lower wavelengths of an MWIR system has a larger depth of focus compared with an imager working in the visible band thus negating the need for an additional focus mechanism. The structure holding the mirrors ideally has the same thermal coefficient of expansion as that of the mirrors, making the system naturally athermal. Choice of low expansion materials (low expansion glass ceramic and Carbon composite / Invar) makes the whole system stable to flight temperature variations, both orbital and seasonal.

Carbon composite has very good properties, being lightweight and can be engineered to have a CTE very close to that of glass ceramic. It does have significant drawbacks in terms of its design complexity, manufacturability (high pre-preg cost and lead time, minimum order costs, limited shelf life, high tooling and lay up cost, limited scalability) and performance (moisture outgassing). Invar structures have the potential to possess adequate stability, whilst being quick to design and analyse, facilitating design flexibility and fast assembly which can be easily scaled for series production.

Historically, Invar structures have suffered from temporal instability with low coefficient of thermal expansion being achieved by quenching the material, locking in residual stress in the structure causing unpredictable distortion. Both these issues have been addressed by selection of Invar alloys with low carbon content which is now readily available, and long term stability is achieved through annealing and artificial ageing of the structure after vacuum brazing.

To achieve the goal of fast design and manufacture DarkCarb has been designed to use an Invar structure and is constructed from simple machined components, drawn tubes and sheet metal parts assembled together using the vacuum brazing process.

The principle structural component is the bulkhead which is made in a closed box section from two shells brazed together. The bulkhead supports the metering truss, the primary mirror and the focal plane structure and provides the mounting interface to the space craft through the imager Anti-Vibration (AV) mounts.

The metering structure is a brazed assembly of components and supports the secondary mirror support structure, Fig. 6.

The focal plane structure shown in shown in Fig. 7 illustrates how the approach allows complex 3D structures to be built rapidly from sheet metal primitives.

The brazed joint can be considered as monolithic with the components joined, making analysis of the structure straight forward, and machining components from solids brings greater flexibility of shape, fastener position, light weighting schemes etc. Long distances within the structure are spanned using precision drawn tubes or sheet metal structures built up from multiple 2D shapes which can be cut accurately and without heat distortion by the water jet process with very short lead times.

Brazing the components together under vacuum at temperatures in excess of 1000°C requires the components to be accurately located and supported, which is achieved through the use of self-jigging features in the components, assembly jigs and brazing jigs.

After brazing, the flight assembly is aged for 2 days at a lower temperature. On removal from the brazing fixture minimal work is required, to prepare it for integration.



*Fig. 6. Primary Truss Structure*

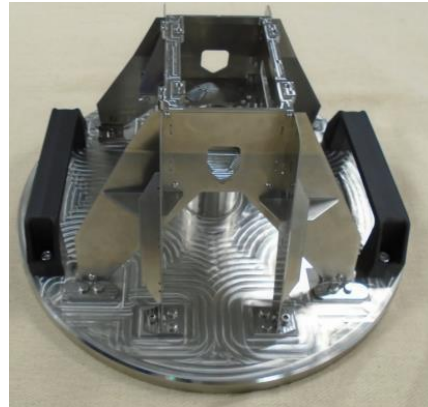


*Fig. 7. Focal Plane Structure*

To validate the structural strengths this concept offers, an Engineering Model imager structure was built and subjected to vibration and shock testing, Fig. 8. After surviving predicted flight loads with no discernible damage, the vibration level was increased to generate stresses at critical joints equal to the yield stress measured in simple pull test sample, and an extended endurance test was run. After the equivalent of 30 minutes random vibration at flight qualification levels, no damage was detected confirming the robust nature of the design.

Use of Invar requires careful attention to mass control, and thermal management provisions. Although the design is predicted to operate without active thermal control of the metering structure, to mitigate the risk of orbital temperature swings being greater than predicted, the imager embodies distributed heaters to regulate the temperature of the metering struts.

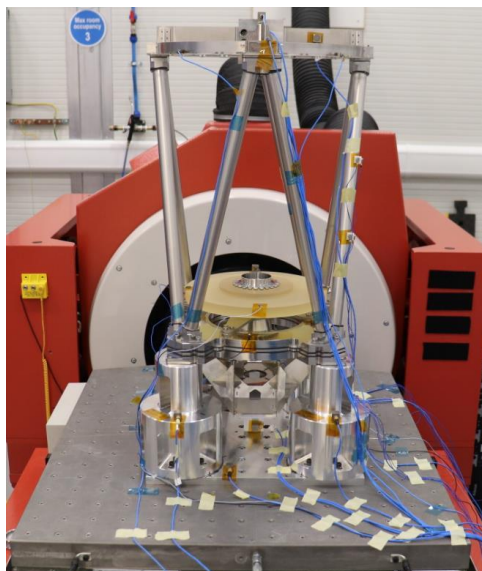


*Fig. 8. DarkCarb EM Structure Vibration Test*



## Calibration System

### The Need for Calibration

The MCT detector used in the DarkCarb imager is made up of an array of pixels, each of which have their own response to incident thermal radiation. The response of each pixel changes slightly for each power cycle of the detector. The different responses of the pixels cause the raw images from the detector to look noise dominant and, although they contain lots of information, it is hidden (see LHS of Fig. 9). The calibration aims to normalise the response of all these pixels so that a clear image can be formed. This is done by imaging a calibration target which can vary in temperature allowing the response curve of each pixel to be established. The raw pixel values can then be converted to an equivalent blackbody temperature when viewing ground images. An example of a calibrated image can be seen on the RHS of Fig. 9. As the response changes for each power cycle the calibration needs to be recalculated each time the detector is powered on to get the most accurate data possible.

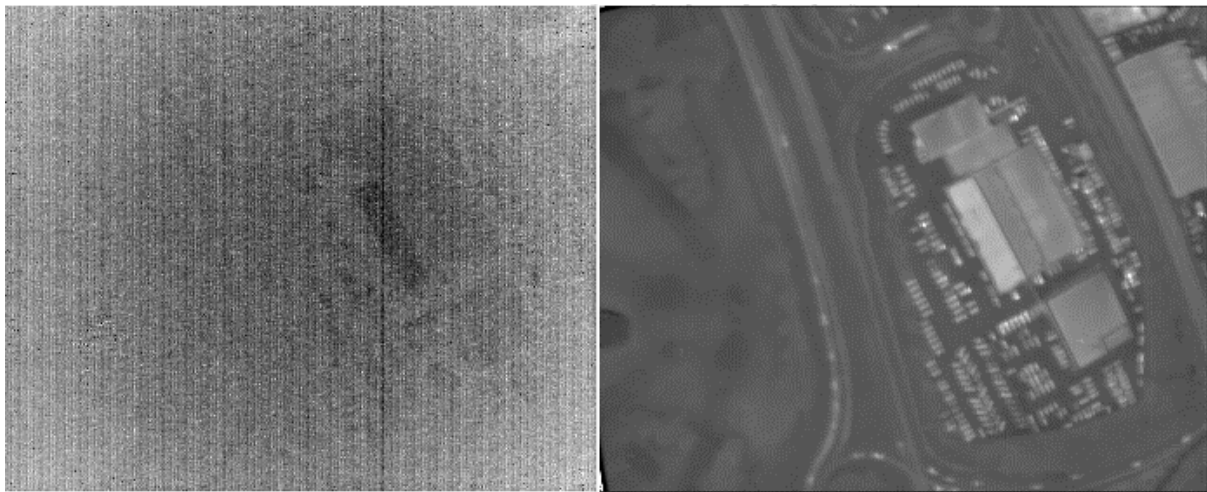


*Fig. 9. Raw and Calibrated Image*

To achieve this, a pair of calibration targets have been incorporated into the design which will be used to calibrate the sensor during each imaging session. These targets should be able to cover the entire operational range of the imager and therefore need to be operational between  $-20^{\circ}\text{C}$  and  $+50^{\circ}\text{C}$ .

### Calibration Wheel

The DarkCarb imager utilises a novel approach to the calibration target design by placing it in the middle of the optical path as opposed to next to the detector or outside the optical materials. The target has been placed in this location for a multitude of reasons, including thermal design, sizing of the mechanism, and the optical performance. The basic idea of the targets is that they are moved into the optical path during calibration (over which time they are heated), and then moved out of the optical path during ground imaging. The design of the calibration wheel which houses these targets is shown in Fig. 10. This wheel also includes a daytime filter and nighttime window which shifts the waveband over which the imager is sensitive depending on viewing conditions. The primary use of these filters is to prevent solar reflections (which mainly occurs under  $4.2\mu\text{m}$ ) during daytime imaging.

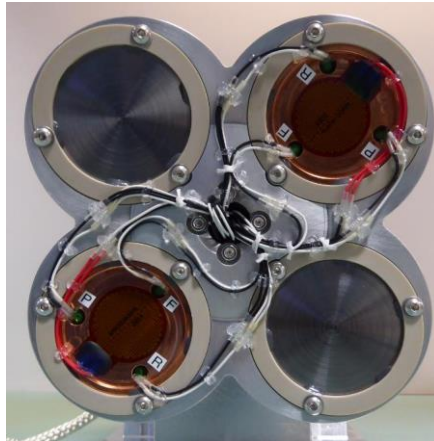


*Fig. 10. EM Calibration Wheel*

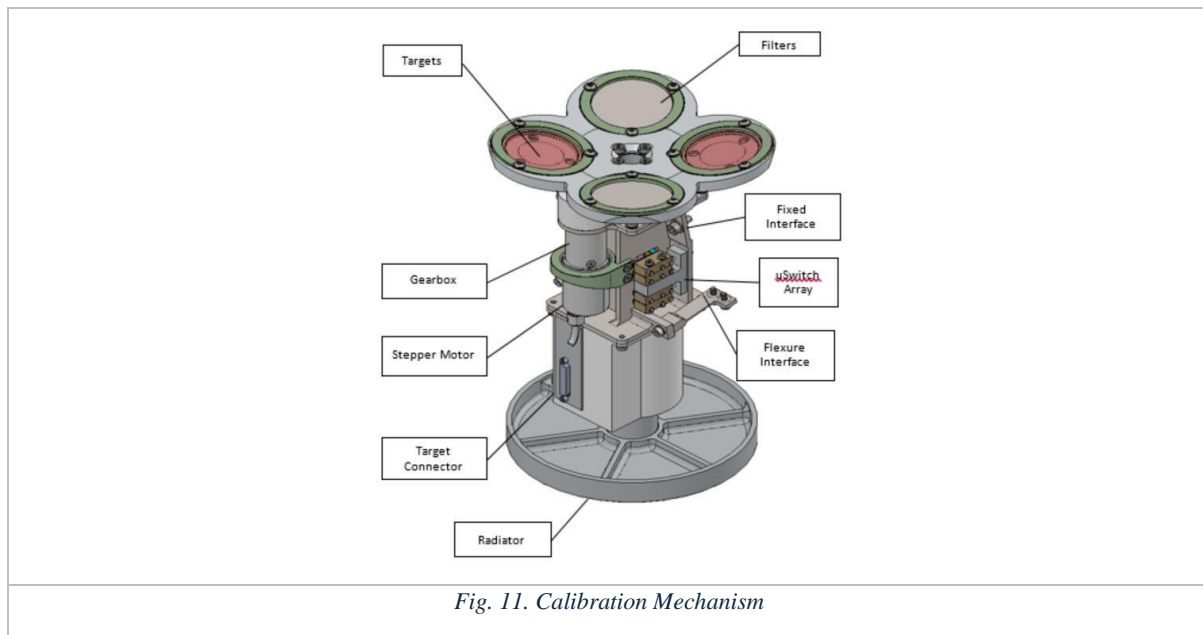
## Calibration Target Design

Within the mechanism the calibration targets have been designed in such a way that during the calibration process they are as thermally isolated from the rest of the spacecraft as possible to ensure they meet the homogeneity requirements. However, after calibration they also need to be able to cool down before the next imaging session. This requirement has influenced the shape, material, and bonding method of the targets. The current design uses copper which is black-etched to provide a suitably emissive surface.

The targets are circular in shape with 2 distinct faces; the back which contains the heating element and temperature sensors, and the front which is black-etched and viewed by the sensor. These two faces are joined by a thin circular extrusion which allows for uniform heat transfer to the front face. The temperature sensors allow for a closed loop control circuit which will dynamically adjust the calibration paddle temperature.

## Calibration Mechanism

The Calibration Mechanism as outlined above serves two purposes on the DarkCarb Imager; its primary purpose is to provide the detector with line of sight to thermal reference surfaces, also known as calibration targets, which are used by the imager to self-calibrate prior to any imaging sessions. The mechanisms' secondary purpose is to provide the optics with a choice of a filter or window, one to use whilst imaging during daylight and the other to use whilst imaging during nighttime.



The mechanism houses two identical calibration Targets and both Filters in a wheel which is rotated by the mechanism in order to place any one of these targets and/or filters into the optical path as required by the imager. This wheel is coupled via a conductive shaft to an external radiator, which provides passive cooling to the Targets throughout the spacecraft's orbit such that they are nominally relatively cold.

SSTL has designed, built, and flown a number of different optical mechanisms throughout its history (N. Phillips et al.). The Calibration Mechanism is unique among these mechanisms as the majority of its design drivers are thermal, which has introduced new challenges and resulted in some unique features being incorporated into the mechanism.

The decision to cool the targets passively was based on a desire for a simple and efficient solution, as active cooling introduces another thermal input and associated complexity. Passive cooling to the level required by the lowest NUC calibration temperature requires an external radiator, which results in a mechanism which is nominal cold compared to the rest of the imager. This requires special attention to lubrication, tolerances, and material selection to ensure that the mechanism does not seize or stall at these low temperatures.

On the other hand, when the calibration Targets are heated to the highest NUC calibration temperature, this can create a temperature difference of up to 70 °C across the mechanism. To manage these gradients, and to facilitate the flow of heat through the mechanism, it employs various thermal management features in the form of thermally isolating spacers, mounts, and flexures as well as thermally conductive gaskets, radiative links in the form of emissive surfaces as well as careful use of multi-layer insulation (MLI) blankets.

The targets are bonded into thermally insulating cups to provide a weak conductive link to the wheel and external radiator such that over an orbit they reach temperatures below the 1<sup>st</sup> NUC temperature. The two targets are identical and provide both a level of redundancy to the imager whilst facilitating double the number of calibration sequences per orbit.

The mechanism is designed to facilitate the rotation of the wheel, shaft, and radiator around their axis. This rotating assembly is supported by a pair of bearings selected to provide a low coefficient of friction at low operating temperatures. The bearings are preloaded against launch loads by means of compliant feature machined into the titanium housing using wire-EDM. This feature also accommodates differing Coefficients of Thermal Expansion (CTE's) between components.

To drive this rotating assembly, a hybrid stepper motor is coupled to a planetary gearbox, which in turn rotates an anti-backlash pinion. This pinion meshes with a spur gear on the main shaft to provide the required motion. An end stop plate attached to the spur gear engages with a dowel on the housing to limit the angle of rotation to just over 300 degrees and also provides a reference position or datum for the mechanism.

Wiring of the heater and sensors on the calibration targets is routed through the rotating central shaft of the mechanism to one end of a Flexi-Rigid Printed Circuit Board (PCB) or 'Flexi'. The other end of this Flexi is mounted to a bracket on the static housing. This allows the electrical connection to the heater and sensors to be maintained through the range of rotation of the mechanism, even at low temperature.

The mechanism uses an array of hall-effect-switches to provide an indication of the position of the wheel. The sensors, motor, heaters, and sensors are all wired to the Services Module electronics, which provide power and control for the functionality of the mechanism.

Finally, the mechanism housing is mounted to the Focal Plane Support Structure of the imager using both fixed and flexure interfaces to minimize the load imparted into this structure due to differential CTE's.

## Electrical System

The electronics for the imager has three main functions. The operation of the detector and acquisition of the image data is served by the detector proximity electronics and the Front End Electronics (FEE). The operation of the calibration mechanism and control of the temperature of the calibration targets is served by the Services Module and the operation and supervision of the cryocooler by the Cryocooler Controller. These three units communicate with the satellite On-Board Computer (OBC) via the CAN bus and are powered directly from the spacecraft 28 V bus.

The MCT MWIR detector is a COTS item and together with two temperature sensing diodes (TSD) are mounted inside the dewar. Two double rows of pins electrically interface the detector to the detector proximity electronics, Fig. 12.

The detector proximity electronics is a single PCB. The main function of this assembly is to convert the analogue outputs of the detector to the digital domain. The detector has eight outputs and these are digitalized with 14-bits resolution and the sampling frequency is 20 MHz. The electrical noise of the video path has been kept low at a few electrons. At the maximum frame rate of 25 FPS, data is generated at the rate of approximately 500 Mbits/s and is transferred to the FEE using high speed Low-Voltage Differential Signalling (LVDS) differential pairs.

A number of linear power supplies provide all the necessary voltage rails and bias to the detector. The output of some of these power rails is adjustable. This is to potentially compensate any end of life radiation effects on the performance of the detector. A number of "housekeeping" Analogue to Digital Converters (ADC) monitor the voltage and current of these power rails together with the temperature of sensors on critical parts of this assembly. These continuously monitor the health of the detector and protect it protect in the event of radiation induced single event latch ups.

Two flexible PCB circuits connect the detector proximity electronics to the FEE. The FEE is a versatile modular unit and its design allows easy integration and adaptation across the carbonite range of mission sensors. It is made up as a stack of four PCBs shown in Fig. 13, a power supply module, a telemetry/telecommands module, a processing module and a detector interface unit. The last one is mission specific and is adapted to serve different detectors used across different types of imagers.

The processing module is designed around a Field Programmable Gate Array (FPGA). This module processes the imagery data from the detector and controls the imaging sequence and timing of both the detector and the ADC. A number of camera parameters can be set before each imaging session. These include the video frame rate, exposure time, detector readout modes (IWR or ITR), low noise or high dynamic range operation and video duration. The processed detector data is packaged in a CoaXPress compatible protocol and transmitted via a dual redundant link to the data recorders.

The Services Module (SM) utilizes a generic design across the mission range providing motor control, heating, and monitoring of other "Services" required to support an imaging payload in Space. This includes a number of LVDS general purpose inputs as well as analogue monitoring and temperature sensor inputs.

A Cryocooler Controller has been developed to ensure the required performance is met in the most demanding conditions. The Cooler Electronics is derived from the heritage SSTL wheel and Antenna Pointing Mechanism (APM) electronics design using SSTLs experience to ensure that the design is fit for a space environment and was based on the electronics design shared with SSTL from Thales Cryogenics, who supplied the Cryocooler for DarkCarb.



*Fig. 12. The Detector Proximity Electronics PCB*



*Fig. 13. Modular Front End Electronics*

## DarkCarb Image Processing

### Non-Uniformity Correction

Non-Uniformity Correction (NUC) is required for all MCT type detectors, it is discussed in more detail in Section 0. The NUC is determined using a set of data captured from the detector while the calibration target is in view of the detector and warming up homogeneously to generate a response curve for each pixel as the temperature of the target increases. The response curve for each pixel is that pixel's response vs the average pixel's response over the whole detector. When the response is linear, a simple Gain and Offset can be applied to each pixel for any image, and theoretically the response of each pixel should then be normalised to provide relative measurements that can be compared to each other. NUC is part of the image processing that SSTL's ground processing performs.

### Flat-Field and Variable TSE Correction

No optical system is perfect, and the uniformity of the image projected onto the detector will vary depending on the optical system. When viewing a completely flat field, one would expect the detector's response to also be flat across the field, however in reality this is not the case, and there is a scaling factor which needs to be applied to every pixel to generate imagery with comparable pixel values across the field. This is performed by capturing images of homogenous targets (ice fields, or views of the ocean at night) and calculating gains is a simple process of adjusting all pixel's values to result in a flat field across the detector.

Thermal Self Emission (TSE) from the imager's optics and mechanics is a contribution to all signals measured at the detector, and TSE has shape and magnitude to it in terms of variation across the detector. As the thermal state of the imager is not under constant control due to power and cost constraints, it is assumed that the TSE contributions to the signal levels at the detector will vary (slowly) over the course of the mission's duration. Frequent flat-fielding activities will result in constantly updated gains to be applied in order to maintain flat field responses to homogeneous scenes.

### Bad-Pixel Correction

Bad-pixels are part of working with MCT detectors – bad-pixels can have varied definitions, but typically they are in one of three different types:

1. Non-Responsive pixels, which can read out constant values, usually at either ends of the response range.
2. Bi-Modal pixels, which can flip between different responsivities at random, and it is not possible to know which state they are in.
3. Noisy pixels, which have an NETD much higher than the average across the detector.



This is an oversimplification but is helpful in understanding how to deal with those bad pixels. For the purpose of HotSat-1, correcting for bad-pixels was not something SSTL had to undertake, but there are various methods one can use from localised averaging to image stacking like that discussed in Section 0. Section 0 discussed the radiometric testing of the complete imager and illustrates the distribution of noisy pixels.

## PFM AIV

### Manufacture

The manufacture of the HotSat-1 DarkCarb imager took place at SSTL from June to December 2022. Manufacture of the optics started prior to this, with SwissOptics™ manufacturing both Primary and Secondary mirrors, and Gooch & Houseco™ manufacturing the lenses for the lens assembly. Artemis™ manufactured the window and filter for the Calibration Wheel.



*Fig. 14. Metering Structure, Optical Tube Assembly*

Fig. 14 shows the imager part-way through manufacture, with the Primary Mirror bonded to its support structure on the bulkhead, and the Secondary Mirror assembly bounded to the top of the brazed truss assembly. Also visible is some of the thermal hardware required to keep the mechanics and optics at safe temperatures throughout the mission lifetime.

The Integrated Detector and Cooler Assembly (IDCA) is shown in Fig. 15, with the COTS Leonardo™ MWIR SuperHawk detector connected to the Thales Cryogenics™ LSF9997 cooler, mounted in SSTL's custom Ground Support Equipment (GSE), prior to integration with the Focal Plane Assembly.

The completed Focal Plane Assembly is shown in Fig. 16, prior to integration with the rest of the optical system and before final detector alignment.

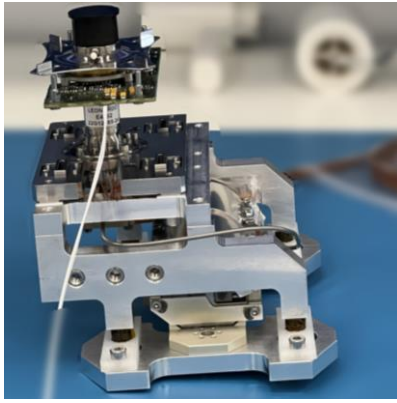


*Fig. 15. Integrated Detector and Cooler Assembly in GSE*

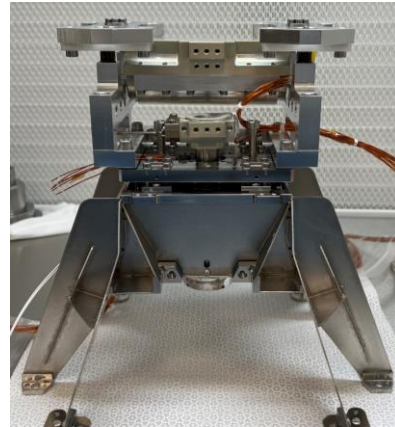


*Fig. 16. Integrated IDCA in Focal Plane Assembly*

Final detector alignment was completed prior to the MTF testing of the imager, using the same GSE and test bench. Placement of the detector at the centre of the optical field was critical to ensure boresight alignment of the imager corresponds to the centre of the detector, likewise, ensuring the detector is flat to the image plane. Sweeping the detector through focus on a hexapod allows for a full characterisation of the focus of the detector, and when measuring at different field angles, this allows for a full map of where the image plane of the optical system is. The detector is then bonded in place and allowed to cure prior to MTF baseline testing. The MTF testing of the imager is discussed in Section 0

The complete DarkCarb imager assembly is shown in Fig. 17, without its Multi-Layer-Insulation (MLI) blanket, prior to integration with the Spacecraft. This image also shown the instrumentation cables (blue) which were installed for vibration testing of the imager at Spacecraft level.



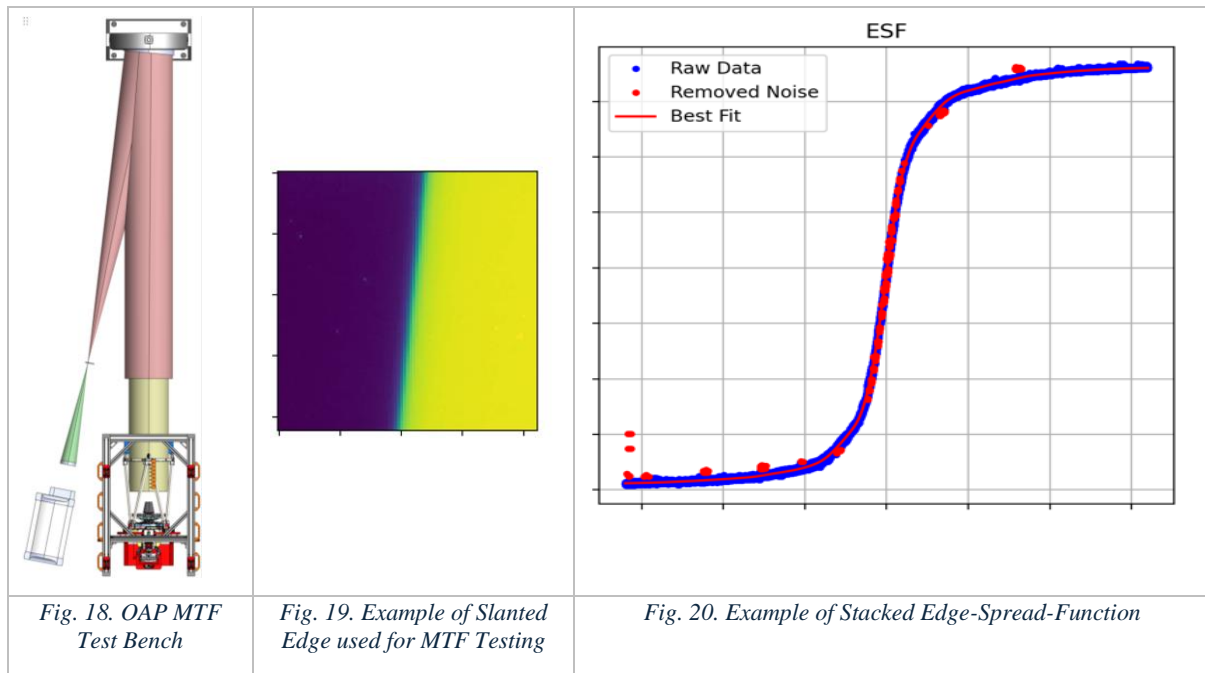
*Fig. 17. Complete Imager with Instrumentation*

After Spacecraft level testing, the imager was removed from the Spacecraft for final system testing, following the same approach as set out in the next two sections.

## MTF On-Ground Testing

The DarkCarb MTF Test Bench at SSTL makes use of a single Off-Axis Parabolic gold-coated mirror, aligned in the visible with an interferometer to within  $\lambda/8$  at 633 nm, providing sufficient performance at the wavelengths in

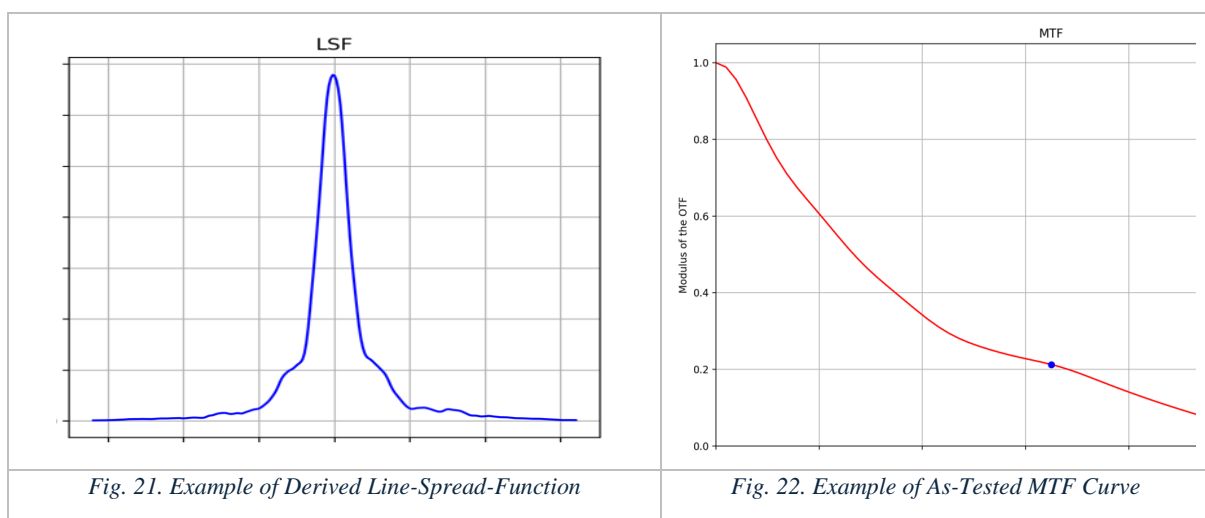
question. The test target (slanted edge) is placed at the focus point of the system and a heated blackbody is placed behind the target to provide the contrast across the edge.



An example of a slanted edge captured during MTF testing of HotSat-1 is shown in Fig. 19, showing the slant of approximately 5 degrees. For protection of Intellectual Property, all scales in subsequent figures have been removed.

To reliably test the MTF of the system, a sequence of 100 images was captured to provide suitable noise-minimising techniques. For each image, the location of the edge was determined analytically using rudimentary image processing techniques. Across all 100 images, a selection of pixels along the length of the line and within a certain normal distance of the edge was plotted on a curve to create an Edge Spread Function (ESF). Note that due to the stacking of images, the resultant ESF contained irregularly spaced samples, as well as some anomalous samples from bad-pixels. Performing some rule-based filtering of data to remove from the ESF, and then using a Kernel based best-fit method, a re-sampled and therefore averaged ESF was created for onward processing. The raw data, removed data, and best fit curve is shown in Fig. 20.

After the smoothed ESF was created, the standard approach of taking the derivative of the ESF to create a pseudo Line Spread Function (LSF) in Fig. 21 was followed, and then the commonly used taking the Fourier Transform and normalising it for both magnitude and effective sampling to produce an MTF curve, Fig. 22.



Note that due to Intellectual Property concerns, the scales of these plots have been removed.

The above image shows an example of an MTF curve generating during on-ground testing of the DarkCarb imager for HotSat-1. There is a point of interest highlighted in Blue, which was used as illustration for the customer to validate the requirements.

## Radiometric On-Ground Testing

The radiometric testing of the DarkCarb imager for HotSat-1 was the final set of optical tests to be performed prior to final delivery to AIT. The radiometric testing consisted of numerous tests while viewing a blackbody placed in the field of view of the OAP MTF test bench. The imager had full view down the optical axis of the OAP, and the blackbody was then placed deliberately out of focus to further smooth out the surface of the blackbody.

The radiometric testing was to fundamentally determine the Thermal performance of the imager, in terms of Noise Equivalent Temperature Difference, which is what temperature (blackbody) the noise in the image represents in terms of uncertainty in any pixel's single response. This is target dependent, and viewing condition dependent, but correlating the on-ground radiometric model would allow for more accurate predictions of what the in-orbit performance would be. NETD is defined as the average temporal noise divided by the average responsivity. We use the term 'average' as each pixel is unique in an MCT detector.

Testing consisted of setting the blackbody to various temperatures equi-spaced from 12°C up to 50°C, and at each temperature taking a set of 512 images for a series of integration times. This allowed a response vs. temperature curve for each integration time to be generate. An example the 512 images' 1024 x 1280 pixels' responses for a constant blackbody temperature is shown in Fig. 23, showing the spread of pixel responses (on a scale from 0 to 16383 – 14-bits) for a constant and homogeneous scene. The average response (mean) is used when plotting the response curve.

At each temperature, and at each integration time, the same dataset is used to determine a corresponding noise vs. temperature curve. The noise value is determined by analysing each pixel across all 512 frames and taking the standard deviation of the 512 values for each pixel. Those standard deviations (1.3 million values) are then plotted on a logarithmic scale curve, shown in Fig. 24. This illustrates the previously made point about the noisy pixels – the logarithmic curve decays down and had a 'tail' on the right of the curve, as these are the noisier pixels' impact on the data. When taking the average from this set of data, it is important to note the difference between the mean and mode of the data – the 'tail' of the data impacts the mean and inflates the noise value, therefore it is more appropriate to use the mode of the data, which is the peak of the curve, and represents the most statistically probably noise value for all pixels across the detector. This mode value is then taken and plotted on the noise vs. temperature curve. With both curves, we now have enough information to determine the NETD curve, which will be both temperature (target) dependent and integration time dependent.

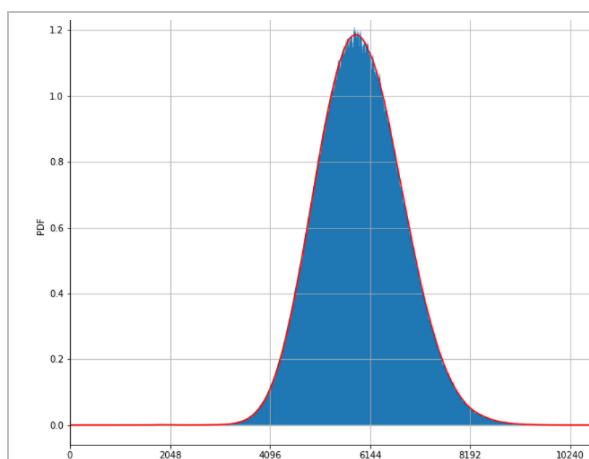


Fig. 23. PSD of Pixel Response to Homogenous Scene

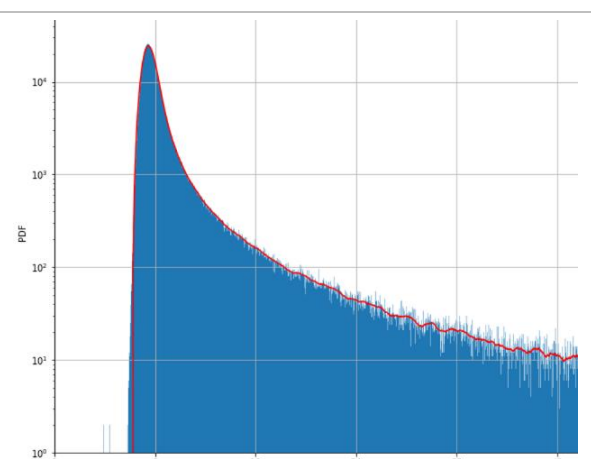
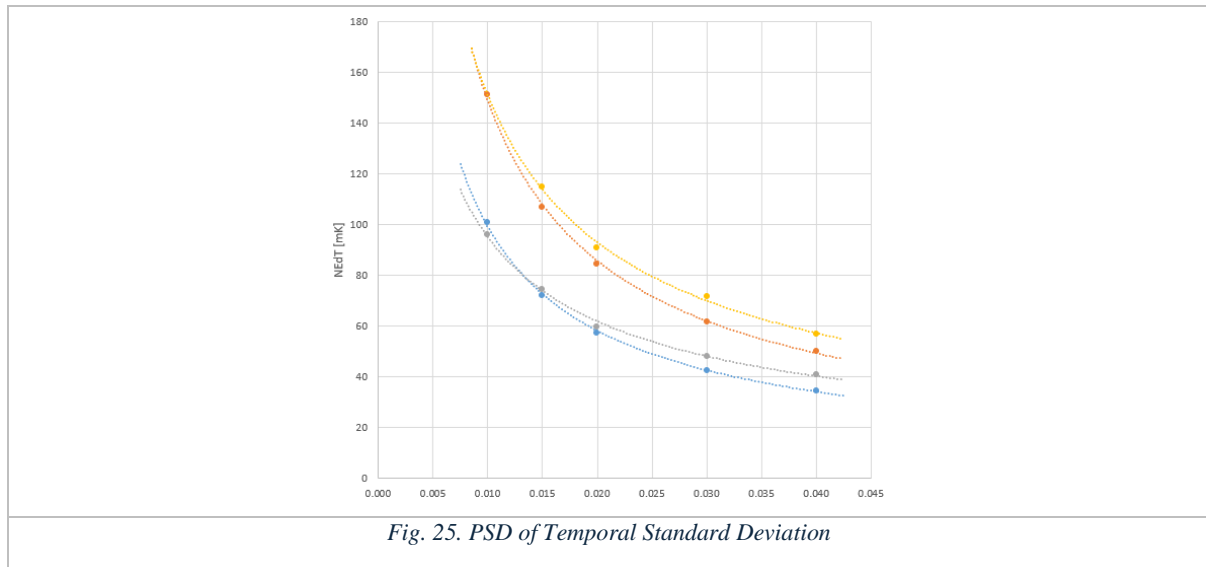


Fig. 24. PSD of Temporal Standard Deviation

The NETD curve for a certain temperature was then compared to the modelled NETD for that same temperature in lab conditions, and the following figure shows the result.



*Fig. 25. PSD of Temporal Standard Deviation*

The integration time is shown on the X-axis, and the NETD is shown on the Y-axis. What the two sets of data represents cannot be explicitly stated for protection of IP, but the yellow and orange datasets are for a set of parameters' modelled and measured values, and the blue and grey datasets are for another set of parameters' modelled and measured values.

The final NETD curve for modelled in-orbit conditions was shared with the customer when closing out the on-ground testing results, and the imager surpassed expectations, with a modelled NETD of between 60 mK and 70 mK for the mission baseline set of parameters and assumptions.

## Launch

HotSat-1 shipped from the UK at the end of April 2023, and then launched on the Falcon-9 Transporter 8 (Fig. 26) on the 12<sup>th</sup> of June 2024. The satellite commissioning was carried out from SSTL's facilities and stations in Guildford. HotSat-1 would have a set of 3 passes in the morning and evening.





*Fig. 26: Transporter-8 - SpaceX*

Following deployment from the launcher, contact was established on the first pass and the spacecraft was then placed into a safe attitude mode. After initial platform safety checks, the solar arrays were then deployed on the second day, after which the propulsion system was commissioned in order to be able to react to possible conjunction warnings.

After satellite platform and payload chain commissioning were completed in the first two weeks, the first image (Fig. 27) was tasked over Rome and shared with the customer, using a NUC calibration dataset captured on-ground during imager ground testing. The resultant image was distinguishable, with known features easily identifiable – green-space naturally emitting less MWIR radiation than built-up areas, with the hot-spot on the left hand side of the image being a St. Peter Square in the Vatican city. Subsequent work was then started to fully calibrate the payload and data-chain. A SatVu image product is shown for comparison on the right-hand side.

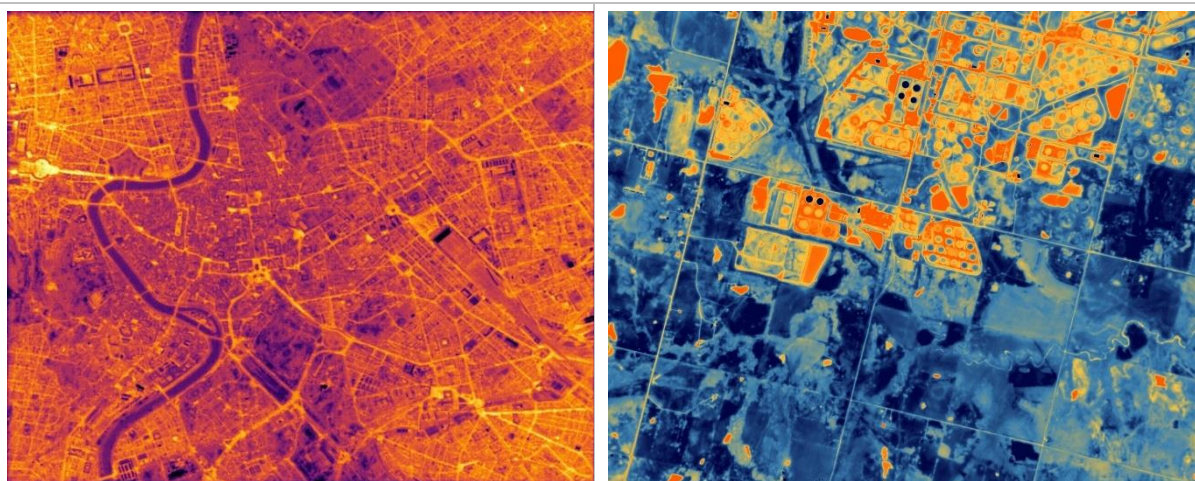


*Fig. 27. First HotSat-1 Image (left), Operational image of oil storage in Cushing, Oklahoma.*

# In-Orbit Performance

## Imager Commissioning

After a successful launch and with a healthy spacecraft system, the task of instrument commissioning began. The first step was to capture in-orbit datasets of calibration data, and to refine the exposure time during calibration runs to capture the maximum range of pixel response values without saturating the detector.

A section of a raw, uncorrected image captured over Atlanta, GA, in Fig. 28, shows the level of detail (or lack thereof) with raw imagery from the MCT detector. Note that the imagery in this section shows higher signal levels as darker regions

Observable in the image above is the Fixed Pattern Noise inherent in the MCT technology, as well as a slight darkening of the image on the left-hand side. This darkening is due to the response of the optical system (and some TSE) which also needs flattening with some flat-field correction.

Applying both the flat-field correction and Non-Uniformity-Correction to the image results in the image shown in Fig. 29. Note that Bad-Pixel correction has not yet been performed at this stage.

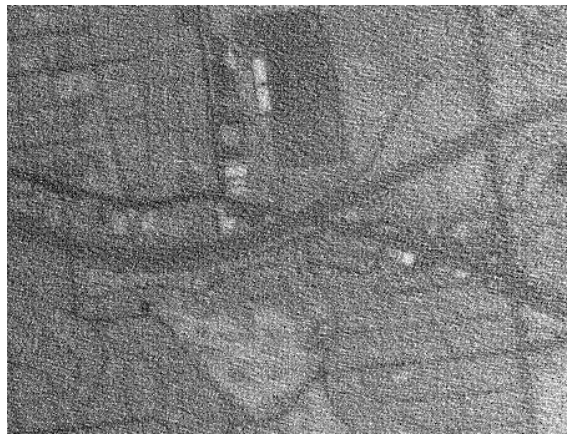


*Fig. 28. Raw Uncorrected Image*



*Fig. 29. Calibrated and Corrected Image*

The resultant image is much more acceptable and was of relatively similar in subjective quality to that of the first images captured Fig. 27, however bad-pixel correction was clearly still required. The detector had many bad-pixels, including a cluster of bad-pixels (outside of the selection shown above).

## Customer Handover

The In Orbit Commissioning Review was completed after 4 months and the spacecraft handed over to Satellite-Vu for commercial operations along with additional imagery and a MWIR video taken by the spacecraft showing a moving train over Chicago published as part of a press release (BBC News).

## Image Stacking Study

Under internal PD funding, SSTL decided to make use of the excellent imagery captured during commissioning and test some quick and rudimentary image-stacking techniques. A set of 40 images were used (more than this and it was found the relative movement of the satellite starts to become a factor) and a method of automatically identifying a common set of features in the image was used – using the movement of the images due to AOCS instability it was possible to remove all bad-pixels from the resultant image, as each area on the ground was sampled sufficiently well by other frames in the sequence. Removal of the bad-pixels, however, was secondary to the primary purpose of the image-stacking, which was to improve the noise in the image, and bring out smaller features that were dominated by the remaining noise in the image after flat-fielding and NUC. By stacking all 40 frames, and then averaging to re-sampling them (and ignoring bad-pixels in the averaging) resulted in the image shown in Fig. 30. This resultant image had significantly better quality than the single image shown in Fig. 29, all bad-pixels had been removed, and it was now possible to make out much more detail in the image. Note the clarity



and detail of the on/off-ramps to the freeway, the central reservations on the freeways, and the noise-free homogeneous regions.



*Fig. 30. Image-Stacking Study Result*

The internal study was very useful in identifying the potential image processing opportunities for the MWIR imagery – and while computationally expensive when performed on an office desktop, the possibilities when going to higher-specification or cloud-based processing becomes very attractive.

## Response

In October 2023, following the successful commissioning and handover of the spacecraft to the customer, the SSTL HotSat-1 project team were honoured by the Arthur C. Clarke Foundation with the 2022 award for Space Achievement by an Industry/Project Team at their Gala dinner concluding the Reinventing Space Conference (11-13 October) in Liverpool, UK.

In December 2023, the SSTL Optical Team was awarded the Royal Aeronautical Society’s Bronze Medal for “the design, development and manufacture of a revolutionary Mid-Wave Infra-Red Thermal Imager used on Satellite Vu’s Pathfinder Satellite.”



*Fig. 31. HotSat-1 Project Team*



*Fig. 32. SSTL Optical Team (credit: RAeS)*

Following successful demonstration of HotSat-1 in-orbit, Satellite-Vu is planning to deploy a constellation of HotSat satellites (SpaceNews) which will address a range of applications for thermal imaging with high spatial and temporal resolution.

# Conclusions

As technology improves, some applications suddenly become viable, and tracking such technologies can provide a significant edge. The DarkCarb development leverages the latest updates in MWIR sensor technology, long-lifetime cooler technologies, and the capabilities of the SSTL Carbonite series of video target tracking satellites. These basic building blocks has led to the quick development and successful demonstration of the first DarkCarb satellite (HotSat-1) and demonstrates that there are still huge opportunities for new commercial space business and applications.

## ACKNOWLEDGEMENTS

SSTL would like to thank SatVu for the right to publish their imagery in this paper, and the list of authors/contributors as well as the wider team at SSTL (past and present) for the hard work and dedication that led to the success of the DarkCarb payload.

## REFERENCES

- BBC News. *Jonathan Amos: HotSat-1: UK spacecraft maps heat variations across Earth*. 6 October 2023.
- C. Weiss et al. "A New Dimension in Small Satellite Constellations." *IAC-19-B4.7.1*. Washington D.C. USA: 70th International Astronautical Congress, 2019.
- D.Cooke et al. "HSDR-X - Design Choices in Maximising Data Returns from Small Satellite Missions." *IAC-20-B4-6A-12*. 71st International Astronautical Congress, 2020.
- Gat et al. "Variable cold stop for matching IR cameras to multiple f-number optics." *SPIE 6542* (2007).
- N. Navarathinam et al. "Carbonite-1: One Year of High Resolution Video Imaging." *IAC-16-B4.6A.1*. Mexico: 67th International Astronautical Congress, 2016.
- . "The Case for Video Imaging from Space." *IAC-16-B4.4.4*. Mexico: 67th International Astronautical Congress, 2016.
- N. Phillips et al. "A Fully Integrated Focus Mechanism for a High Resolution Camera." Bilbao, Spain: 16th European Space Mechanisms and Tribology Symposium, 2015.
- SpaceNews. *SatVu aims to revive thermal imaging business in 2025 with two satellites*. 15 May 2024.